EPD Congress 2016
Edited by: Antoine Allanore, Laura Bartlett, Cong Wang, Lifeng Zhang, and Jonghyun Lee
TMS (The Minerals, Metals & Materials Society), 2016

LASER ABLATION OF ALUMINUM AND TITANIUM ALLOYS UNDER GLASS CONFINEMENT

Peixuan Ouyang[1], Liangju He[2], Peijie Li[1, 3]

[1]Department of Mechanical Engineering, Tsinghua University, Beijing, 100084, China
[2]School of Aerospace, Tsinghua University, Beijing, 100084, China
[3]National Center of Novel Materials for International Research, Tsinghua University, Beijing, 100084, China

Keywords: Laser ablation, Gap width, Laser intensity, Crater profiles, Crater morphologies, Phase explosion.

Abstract

Single-pulse laser ablation of aluminum and titanium alloys under glass confinement is investigated. Processing parameters such as laser intensity and gap width between targets and glass are varied. Surface morphologies and crater profiles of the alloys after laser ablation are studied by SEM and white-light interferometric microscope, respectively. The effects of gap width and laser intensity on surface morphologies and crater profiles of targets are systematically analyzed. In addition, the generation of porous surface structures in Ti target is regarded as the result of phase explosion in the molten surface layer of targets and the thermodynamic condition in our experiment for phase explosion is evaluated.

Introduction

Pulsed-laser ablation of solid substrates under the confinement of transparent glass has shown great potential in laser shock peening (LSP) [1], nanoparticle deposition [2], laser shock cleaning (LSC) [3] and generation of porous metal surface for chemical and electrochemical application [4]. The laser-induced plasma is effectively confined between the target surface and the glass overlay such that strong shock wave is generated acting on the targets. Thus, laser intensity and gap width between target surface and glass greatly affect the shock wave pressure and the processing results of targets. In order to have better understanding and full application of glass-confined laser ablation, the effect of the gap width and the laser intensity on laser ablation process is investigated respectively.
Two modes of laser ablation were used in our work. One is “semiconfined ablation”, which is first proposed by Lugomer [4], in which a laser beam irradiates the target through a transparent glass positioned slightly before the target surface. In this experimental configuration, the effect of the gap width on laser ablation of Al alloy is investigated. The other one is “confined ablation”, in which no gap exists between the glass and the target. In this experimental configuration, the effect of laser intensity on laser ablation of Al and Ti alloys are studied.

Experimental Procedures

The experimental setup of “semiconfined ablation” and “confined ablation” are shown in Fig. 1a and Fig. 1b, respectively. For the “semiconfined ablation” experiment, aluminum 5A06 alloy

(referred to as Al target in the following) was irradiated using a Q-switched Nd:YAG laser (wavelength λ=1064 nm, pulse duration τ=10 ns, intensity I~7.5×10^{10} W/cm^2) at single-pulse mode. The gap width between targets and glass was controlled through transparent tapes with monolayer thickness of 350 m as spacers. For the "confined ablation" experiment, no transparent tapes exist between targets and glass. Al alloy and titanium TB5 alloy (referred to as Ti target in the following) were irradiated by a single laser pulse at combined wavelengths of 1064 nm and 532 nm with total intensity ranging from 7.5×10^{10} W/cm^2 to 3.7×10^{11} W/cm^2. For both semiconfined and confined experiments, soda lime glass slides with thickness of 1 mm were used. Rectangular shaped targets with thickness of 1 mm were grinded and then cleaned with distilled water and acetone before laser ablation.

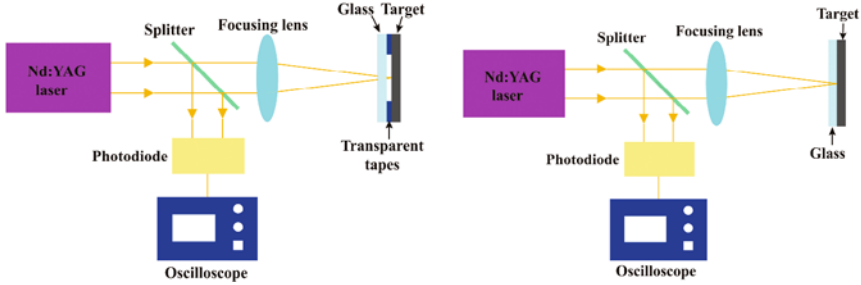

Fig. 1. Experimental setup. (a) "semiconfined ablation"; (b) "confined ablation".

After laser ablation, the targets were cleaned using ultrasound cleaning in acetone for 15 min and in alcohol for 5 min. The surface morphologies of produced craters were investigated using Scanning Election Microscope (Hitachi-S4800). The cross-sectional profiles of craters were measured through white-light interferometric microscope (MicroXAM-3D) with horizontal and vertical resolutions of 0.11-8.8 m and 0.01 nm, respectively. The depth of craters is defined as the distance between the horizon at level zero and the lowest point on the crater profiles. For the case of semiconfined experiment, the back side surfaces of glasses after laser irradiation were observed using optical microscopy.

Results and Discussion

Effect of Gap Width on Laser Ablation of Al Alloy ("Semiconfined Ablation")

Fig. 2 shows surface morphologies of craters in Al target induced by glass-semiconfined ablation with different gap widths. For the crater induced with the gap width of 1.4 mm, re-solidification structure with slight and disordered liquid movement is observed (Figs. 2a and 2d). For the crater induced with the gap width of 700 m, more intensive but still disordered liquid wave is presented (Figs. 2b and 2e). While for the crater induced with the gap width of 350 m, strong radial liquid jets and strings of drops broken from liquid jets due to the instability of jets [4] are formed in the ablated area (Fig. 2c), and slightly porous surface with micro-cavities regarded as bubble nucleation sites [5, 6] appears in the central part of the crater (Fig. 2f). With the gap width decreasing, space becomes very limited for expansion of the ablated plasma, resulting in the formation of high-temperature-high-pressure plasma disk trapped between the target surface

and the glass [4]. As a result, bubble nucleation is prone to occur and strong shock wave induced by hot plasma acts on the molten pool of targets, leading to the morphologies shown in Fig. 2c and 2f.

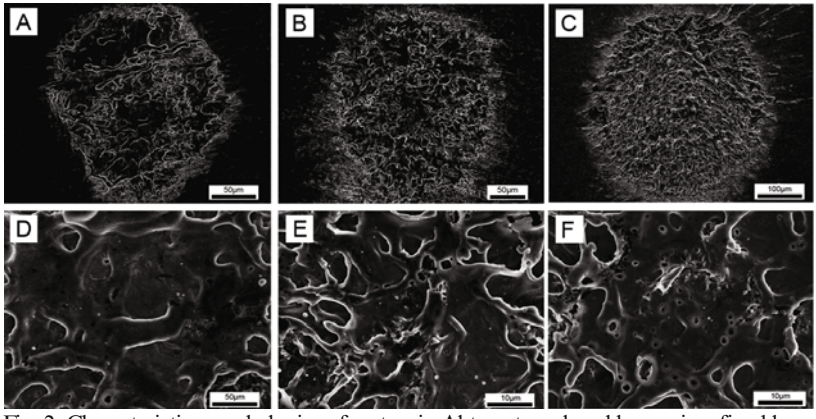

Fig. 2. Characteristic morphologies of craters in Al target produced by semiconfined laser ablation with different gap widths. From left to right, the corresponding gap width is 1.4 mm, 700 m and 350 m. The top row shows overall view of the craters, and the bottom row presents the center of the craters.

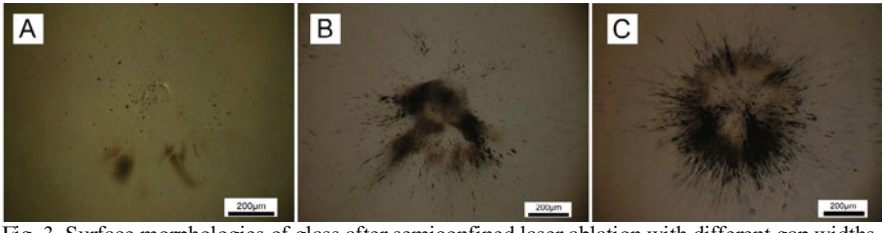

Fig. 3. Surface morphologies of glass after semiconfined laser ablation with different gap widths. (a) 1.4 mm; (b) 700 m; (c) 350 m.

The morphologies of back side surfaces of glasses after semiconfined ablation are shown in Fig. 3. Little damage can be observed in the glass for the ablation experiment with gap width of 1.4 mm (Fig. 3a). With the gap width decreasing, damage in the glass becomes serious. Fig. 3b shows some liquid jets spread from a spot along radius on the glass surface for the experiment with gap width of 700 m, while more radial liquid jets presents on the glass for the experiment with gap width of 350 m (Fig. 3c), which also demonstrates that the shock wave pressure increases with the gap width decreasing.

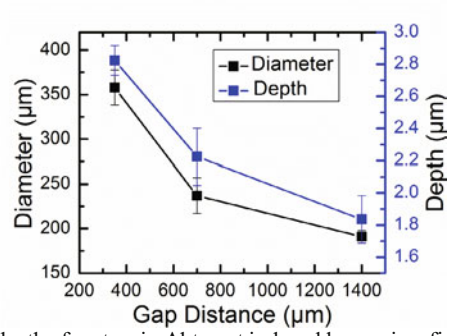

Fig. 4. Diameter and depth of craters in Al target induced by semiconfined laser ablation as a function of gap width.

Fig. 4 presents diameter and depth of the craters in Al target after semiconfined ablation as a function of gap widths. With the gap width increasing, both the diameter and depth of the craters decrease, consistent with coupling coefficient decreasing with gap width increasing [7]. The sizes of crater diameter and depth are closely related to the dynamics and geometry of plasma-induced shock wave which is affected by the gap width between the target surface and the glass [3, 4]. When the gap width decreases from 1.4 mm to 350 m, the shock wave pressure acting on the target increases significantly [3] and the geometry of the shock wave evolves from oblate spheroid to cylindrical slab [4], which implies that the generation of a quasi-two-dimensional shock wave. Subsequently, more materials would be removed from the targets by the shock wave such that craters with large diameter and deep depth are formed when the gap width decreases.

Effect of Laser Intensity on Laser Ablation of Al and Ti Alloys ("Confined Ablation")

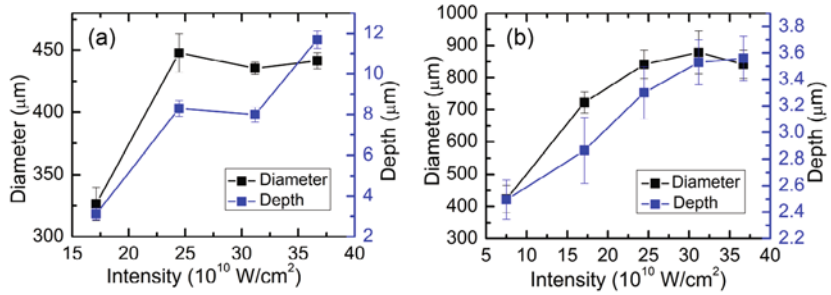

Fig. 5. Diameter and depth of craters produced by glass-confined laser ablation as a function of laser intensity. (a) Al alloy; (b) Ti alloy.

Glass-confined laser ablation of Al and Ti alloys was carried out with the laser intensity ranging from 7.5×10^{10} W/cm^2 to 3.7×10^{11} W/cm^2. Since the crater in Al target induced with laser intensity of 7.5×10^{10} W/cm^2 is unapparent due to the low laser intensity, the diameter and depth

of this crater is ignored in the analysis. Fig. 5 demonstrates diameters and depths of craters induced by glass-confined ablation as a function of laser intensity. For Al target, the crater diameter tends to become saturated when the laser intensity is greater than 2.45×10^{11} W/cm^2, but the crater depth still have a rapid increase when the laser intensity ranges from 3.1×10^{11} W/cm^2 to 3.7×10^{11} W/cm^2 even though the crater depth tends to be stable in the range of the laser intensity from 2.45×10^{11} W/cm^2 to 3.1×10^{11} W/cm^2. For Ti target, the crater diameter increases with the laser intensity increasing but slightly decreases when the intensity is greater than 3.1×10^{11} W/cm^2, while the crater depth of Ti target keeps increasing when the laser intensity ranges from 7.5×10^{10} W/cm^2 to 3.7×10^{11} W/cm^2. It is concluded that the crater diameter is easier to reach a saturated value than the crater depth with the laser intensity increasing, which could be explained by that the shock wave is more effective in increasing the depth rather than the width [8]. Consequently, crater depth could be more representative than crater diameter as a function of laser intensity for both Al and Ti alloys.

Nevertheless, it is worth noting that with the same laser intensity and the same spot size, the crater depth of Ti target is much smaller than that of Al target while the crater diameter of Ti target is greatly larger than that of Al target. Since Al alloy has a lower melting temperature and a higher thermal penetration depth ($\delta_T = \sqrt{\alpha t_p}$, where α is the thermal diffusion coefficient and t_p is the pulse width of the laser beam) than Ti target, a thicker molten surface layer is produced in Al target instead of Ti target and a deeper crater would be generated after the recoiled pressure acting on the molten layer. As for the phenomenon of the crater diameters, it is probably because greater shock wave pressure is generated during laser ablation of Ti alloy rather than Al alloy. According to Fabbro's theory [9], the maximum shock wave pressure generated during confined laser ablation is given by the following relation:

$$P(\mathrm{GPa}) = 0.01\sqrt{\frac{\alpha}{\alpha+3}} \times \sqrt{Z(\mathrm{g\cdot cm^{-2}\cdot s^{-1}})} \times \sqrt{I_0(\mathrm{GW/cm^2})}\,, \qquad (1)$$

where α is the fraction of internal energy devoted to thermal energy (typically α=0.1), I_0 is the incident power intensity, and Z is the reduced shock impedance between the target and the liquid medium, which is defined by the relation:

$$\frac{2}{Z} = \frac{1}{Z_{\mathrm{glass}}} + \frac{1}{Z_{\mathrm{target}}}\,, \qquad (2)$$

where Z_{glass} and Z_{target} are the acoustic impedances of glass and target respectively. Since the acoustical impedance of Al (1.5×10^6 g cm^{-2} s^{-1}) is smaller than that of Ti (2.7×10^6 g cm^{-2} s^{-1}), and the incident laser intensity reaching the surface of Al target is lower than that of Ti target due to the higher reflectance of Al, the maximum shock wave pressure generated in laser ablation of Ti is larger than that of Al, which results in craters with larger diameter in Ti target than that in Al target.

Fig. 6 shows characteristic morphologies of craters in Al target produced by glass-confined ablation with two laser intensities of 1.7×10^{11} W/cm^2 and 3.7×10^{11} W/cm^2. Compared with the crater induced with the laser intensity of 1.7×10^{11} W/cm^2 (Figs. 6a and 6c), the crater generated with the laser intensity of 3.7×10^{11} W/cm^2 presents intensive radial liquid jets moving outwards

(Figs. 6b and 6d), which indicates that a stronger shock wave is generated when laser intensity increases. Fig. 7 presents characteristic morphologies of craters in Ti target after confined laser ablation with three intensities of 7.5×10^{10} W/cm^2, 1.7×10^{11} W/cm^2 and 3.7×10^{11} W/cm^2. From the overall view of these craters (Figs. 7a-7c), it is clear that the crater diameter of Ti target greatly increases with laser intensity increasing. As for the detail view of the center of the craters, more micro-cavities, liquid jets and droplets are formed in the crater when the laser intensity increases from 7.5×10^{10} W/cm^2 to 1.7×10^{11} W/ cm^2 (Figs. 7d and 7e), which is ascribed to the molten layer with high temperature and strong recoiled shock wave due to the increasing incident laser energy. Note that the morphology of the crater generated with the laser intensity of 3.7×10^{11} W/cm^2 (Fig. 7f) is much different from that of the other two craters (Figs. 7d and 7e). The corresponding magnified SEM micrograph is shown in Fig. 8. Smaller cavities are formed inside the larger ones through a series of bubble generation and the cascade of bubble explosion, the phenomenon of which is belonged to phase explosion [4].

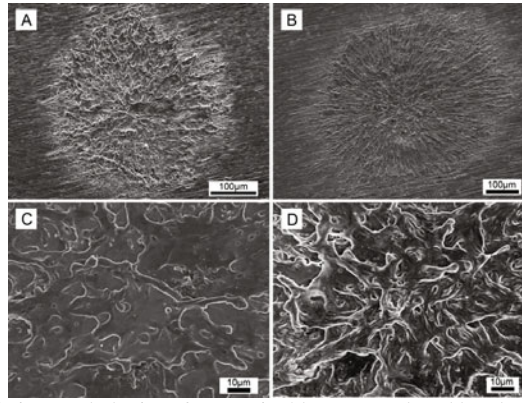

Fig. 6. Characteristic morphologies of craters in Al target produced by glass-confined ablation with different laser intensities. (a) and (c): I=1.7×10^{11} W/cm^2 ; (b) and (d): I=3.7×10^{11} W/cm^2. The top row shows overall view of the craters, and the bottom row presents detail view of the craters.

It is noteworthy that with the same laser intensity of 3.7×10^{11} W/cm^2, phase explosion only occurs in Ti target instead of Al target even though Al target has a lower critical temperature (5410 K) than Ti target (7890 K). There are three possible reasons for this phenomenon. Firstly, Al target has higher reflectivity to laser beam than Ti target such that less laser energy could reach the target surface. Secondly, owing to lower boiling temperature (2600 K) and lower ionization potentials (E_1= 5.98577 eV) of Al than those of Ti (3533 K and E_1= 6.8282 eV), denser plasma is inclined to be generated on Al target rather than on Ti target, resulting in less laser energy reaching the Al target surface through energy absorption of plasma. Thirdly, since much thicker molten surface layer is generated in Al target rather than in Ti target as aforementioned, it is more difficult for Al target than Ti target to heat all the liquid in the molten pool to near critical temperature for the occurrence of phase explosion.

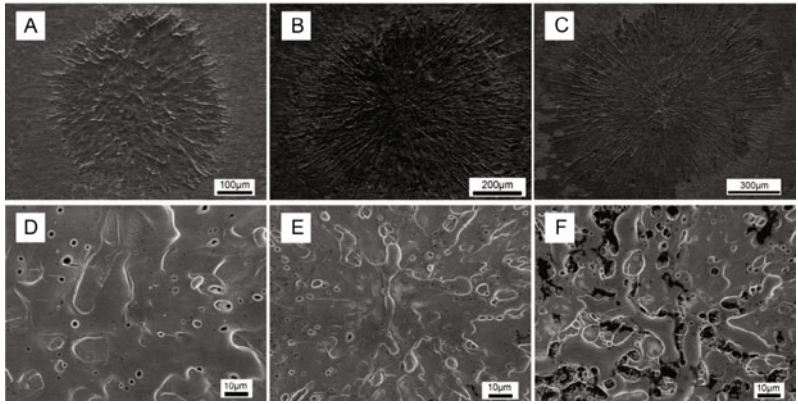

Fig. 7. Characteristic morphologies of craters in Ti target produced by glass-confined ablation with different laser intensities. (a) and (d): I=7.5×10^{10} W/cm^2 ; (b) and (e): I=1.7×10^{11} W/cm^2; (c) and (d): I=3.7×10^{11} W/cm^2. The top row shows overall view of the craters, and the bottom row presents detail view of the craters.

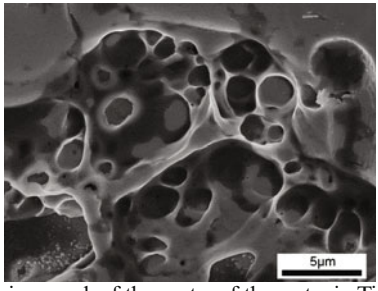

Fig. 8. Magnified SEM micrograph of the center of the crater in Ti alloy produced by glass-confined ablation with laser intensity of 3.7×10^{11} W/cm^2 (Fig. 7f).

Conclusions

In this work, two modes of laser ablation were carried out. One is the glass-semiconfined laser ablation of Al alloy using laser beam with the wavelength of 1.064 m, the other one is the glass-confined laser ablation of Al and Ti alloys using laser beam with the combined wavelengths of 532 nm and 1.064 m.

For semiconfined laser ablation, the crater profiles (depth and diameter) and the morphologies are closely related to the gap width which significantly influences the confinement degree on plasma. The smaller the gap width is, the stronger confinement on plasma is, and so is the shock wave. The diameter and depth of craters increase with the gap width decreasing.

For confined laser ablation, it is shown that the crater depth is more representative than the crater diameter as a function of laser intensity. With the same laser intensity and the same spot size, the

depth of craters in Ti target is much smaller than that in Al target while the diameter of craters in Ti target is much larger than that in Al target. Besides, phase explosion occurs in Ti target instead of Al target with the laser intensity of 3.7×10^{11} W/cm^2.

Acknowledgements

The work was supported by a Tsinghua Scholarship for Overseas Graduate Studies. The authors also want to thank N.E. Kask for providing the laser device and giving good advises in experimental design.

References

1. X.Q. Wu, Z.P. Duan, H.W. Song, Y.P. Wei, X. Wang, C.G. Huang, "Shock pressure induced by glass-confined laser shock peening: Experiments, modeling and simulation," *J. Appl. Phys.*, 110 (2011) 053112 (053117 pp.)-053112 (053117 pp.).
2. T. Donnelly, J.G. Lunney, "Confined laser ablation for single-shot nanoparticle deposition of silver," *Appl. Surf. Sci.*, 282 (2013) 133-137.
3. J. Deoksuk, O. Joon Ho, L. Jong-Myoung, K. Dongsik, "Enhanced efficiency of laser shock cleaning process by geometrical confinement of laser-induced plasma," *J. Appl. Phys.*, 106 (2009) 014913 (014917 pp.)-014913 (014917 pp.).
4. S. Lugomer, B. Mihaljevic, G. Peto, A.L. Toth, E. Horvath, "Spongelike metal surface generated by laser in the semiconfined configuration," *J. Appl. Phys*., 97 (2005).
5. R. Karimzadeh, J.Z. Anvari, N. Mansour, "Nanosecond pulsed laser ablation of silicon in liquids," *Applied Physics a-Materials Science & Processing*, 94 (2009) 949-955.
6. V. Craciun, N. Bassim, R.K. Singh, D. Craciun, J. Hermann, C. Boulmer-Leborgne, "Laser-induced explosive boiling during nanosecond laser ablation of silicon," *Appl. Surf. Sci*., 186 (2002) 288-292.
7. Z.Y. Zheng, J. Zhang, Z.Q. Hao, X.H. Yuan, Z. Zhang, X. Lu, Z.H. Wang, Z.Y. Wei, "The characteristics of confined ablation in laser propulsion," *Chinese Physics*, 15 (2006) 580-584.
8. M.H. Mahdieh, M. Nikbakht, Z.E. Moghadam, M. Sobhani, "Crater geometry characterization of Al targets irradiated by single pulse and pulse trains of Nd:YAG laser in ambient air and water," *Appl. Surf. Sci.*, 256 (2010) 1778-1783.
9. R. Fabbro, J. Fournier, P. Ballard, D. Devaux, J. Virmont, "Physical study of laser-produced plasma in confined geometry," *J. Appl. Phys*., 68 (1990) 775-784.